CFD ANALYSIS ON DART PAPERPLANE

Hazim Sharudin[1], N. I. Ismail[2]*, M. Hisyam Basri[2] and Nur Afizah Jamiri[2]

[1]Mechanical Engineering Studies, College of Engineering, Universiti Teknologi MARA, Johor Branch, Pasir Gudang Campus, Johor, Malaysia

[2]Mechanical Engineering Studies, College of Engineering, Universiti Teknologi MARA, Pulau Pinang Branch, Permatang Pauh Campus, Pulau Pinang, Malaysia

*Corresponding email: iswadi558@uitm.edu.my

Article history
Received
14th June 2024
Revised
25th September 2024
Accepted
5th November 2024
Published
29th December 2024

ABSTRACT

This research aims to analyze the aerodynamic performances surrounding paper planes. The dart paper plane model was chosen for this work based on the availability of experimental work done by previous researchers. The dart paper plane can be categorized as one of the micro air vehicles (MAV), however, the basic aerodynamic performances have been underestimated by previous researchers and are still open to be explored. In this work, a CFD simulation study on the dart paper plane was utilized by using the ANSYS-CFX module platform. A steady state, incompressible flow Navier-Stokes equation (RANS) combined with the Shear Stress Turbulence (SST) model was used to analyze the flow structure over the dart paper planes. Experimental data availability is used to compare experimental and our simulation results. Based on the validation work, the highest average percentage difference between $C_{Lmagnitude}$, C_{Lmax}, and AOA_{stall} between our results and the experimental ones is 11.9%, 29.5%, and 24.2%. However, overall CL trends similarly exhibited with experimental results since the average percentage difference of C_{Lincre} magnitude is continuously reduced from 6.48% to 0.9% towards increment of AOA. For drag performance analysis, the overall trend magnitude distribution of our simulation and experimental results consistently increases towards the increment of AOA. The massive C_D distribution had overcome the consecutive C_L generation, thus decreasing the overall C_L/C_{Dmax} magnitude.

Keywords: *Dart paper plane model, Aerodynamic performances, micro air vehicle, CFD simulation.*

1.0 INTRODUCTION

Paper plane is an origami toy invented for so long, but it is more toward flying applications. The words origami is from Japanese art, which means folding paper [1]. The Japanese art of this paper folding has inspired an aeronautical engineer for designing the innovations of contemporary folded shapes with functional applications. An origami of paper plane has their advantages which has the lightweight and flexible material with good tensile performance [2]. The standards of designing the paper plane is parallel to Micro Air Vehicle (MAV) design which built based on lightweight material stock, but it offers different in process design application. There are five basic designs of the MAV application which are flapping, fixed, membrane flexible, rotary and morphing. In this research, the focus is more on delta fixed wing origami design which is dart paper plane.

The MAV applications are investigated through biological designs that required complex processing to copy for determining their aerodynamics performance [3]. Many researchers are focused on designing the low Reynolds number of the MAV applications since the high Reynolds number are not applicable. The process is still slow since the biological mechanism required is a complicated process to copy. Due to its simplicity, paper planes offer a simple design process and being tested by researcher in recent MAV development. Moreover, since MAV are flying in the same Reynolds number regime as a paper plane, paper planes were the preferred choice due to their simple design and low cost material [4,5]. The simple technique in the design process gives an advantage for the paper plane to be applied in a huge number of design cycles in-flight applications, requiring low aspect ratio (LAR) with low Reynold number for the design [6].

Table 1: Dart Paper Plane Design Requirement [6]

Specification	Requirement	Details
Thickness	0.2 mm	A4 thickness paper
Span	160 mm	Distance tips
Wing Area (S)	20000 mm^2	Shape of wing size
Chord Length (*c*)	250 mm	Distance from leading edge to trailing edge paper plane
Leading edge sweep angle	75^o	Blade row
Aspect Ratio	1.28	Low
Weight	~5 g	A4 paper weight
Speed	5 m/s	Initial Speed
Angle of Attack (AOA)	5^o	Reference line (Longitudinal)

Dart paper plane model is chosen due to the availability of experimental data. The design can be achieved by folding the paper based on the specifications Table 1 that has been suggested by S.Gurnani and M.Damodaran [6]. The dart paper plane design has same as cropped delta wing as prior studies with the advantage of producing high lift coefficient at low Reynolds numbers [7]. According to Schülter, the advantage of dart paper plane design chosen has the high sweep angle (Λ=75^o) which can produce the high lift coefficient at very high angle of attack. The design of delta wing can also produce a vortex structure in continuous manner [8]. Other than that, it has been used in wide range of design cycle due to their simplicity, so it has inspired many aeronautic engineers to use paper as a source of their idea.

In terms of the type of paper plane, it still has an infinite number of variations in their design. Basically, the standard design for paper planes can be categorized as a fixed wing airplane. According to Cook, there are several criteria highlighted to limit the huge number of paper plane design for experiment purpose [9,10]. However, it still left the large scope to design the possible paper plane in terms of aeronautic applications. Therefore, the study on the paper plane are still open to be explored. There are several examples of paper planes based on their performances, stability and popularity in experimental work such as Suzanne Paper Plane, Conventional Dart Paper Plane, The Stable Paper Plane and Ring Paper Plane. Suzanne paper plane has the design wing that low aspect ratio (LAR) and had a dropped delta wing at the wing tips [11]. While the conventional Dart Paper Plane has a design that famous among the researcher due to its popularity in research work [12,13]. The design of dart paper wing usually low aspect ratio (LAR) that operating at LAR= 1.1. The weight of the paper plane is approximately 5g and the sweep angle is 67^o [14]. The Stable paper plane's design has a low aspect ratio (LAR), so it has a maximum value of lift coefficient at the high angle of attack. The high value of the lift coefficient will lead to the stability of the plane while flying [15,16]. The Ring paper plane also have a good lift, stability and aerodynamic performance based on the diameter of the ring. This has been shown based on previous study of the design configuration ring paper plane [17].

Paper planes have been invented long ago but more toward toy applications. Paper planes offer less weight and cost effectively which can be fold based on standard origami technique for any desired shape. So, it is used as trial-and-error for many design cycles [18,19]. It is a parallel concept to the Micro Air Vehicle (MAV), which is required to design using the less weight material. Still, it is challenging due to the actual process of fabricating the aerodynamic structure are too complicated to copy [20]. Since the paper plane can fly the same as the MAV class based on aspect ratio value, it has never been adopted to be MAV because of the lack of understanding of aerodynamic paper planes. In previous study by M. Chang et al., the designs of dart paper plane with the centerfold will creates a secondary flow of the wing vortex inwards which can influence unsteady aerodynamics flow field of the paper planes [9]. However, the aerodynamics performance of dart the paper plane regarding the low aspect ratio wings operating at low Reynolds numbers being underestimated by the previous researcher and still open to be explored. Thus, the present works of dart paper plane carried out in this study.

2.0 METHODOLOGY

2.1 Computational Method and 3D Simulation

The study of paper plane characteristic has included the investigation details of aerodynamic performance and the flow behavior (vortex structure) surrounding the dart paper plane. The computational modeling of paper plane is essential as it is capable to accurately stimulate and analyze of the dart paper plane model in comparison with the available experimental data [8]. The present high sweep angle and centerfold will influence the stall angle of attack paper plane. In return, the paper characteristic on the wing structure also contributes to the change of airflow behavior. Therefore, in order to ensure an acceptable correlation between aerodynamics performance and flow structures, ANSYS CFX simulation is implemented.

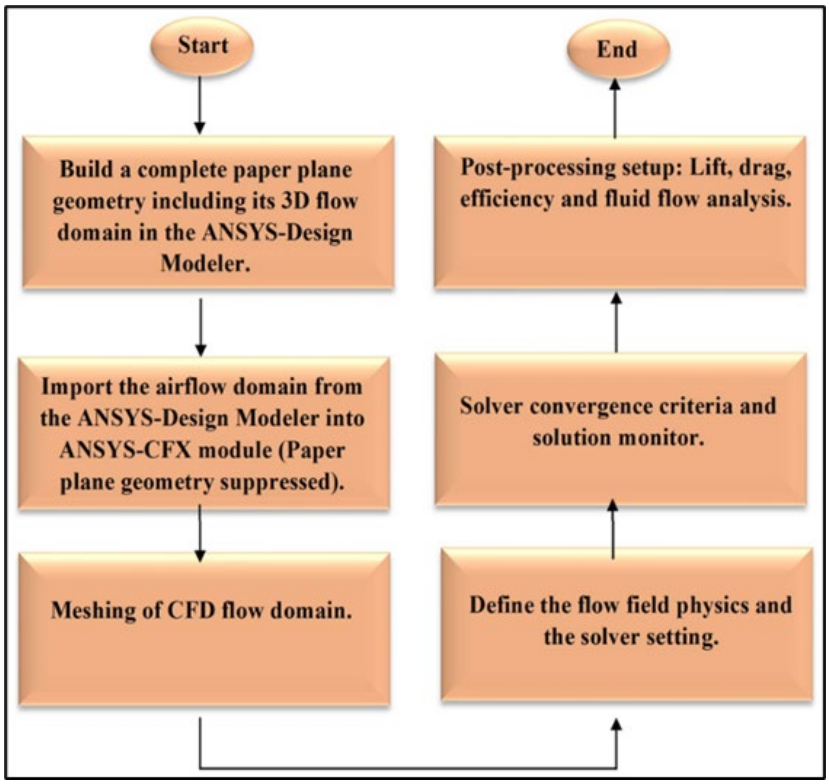

Figure 1: ANSYS- CFX Simulation setup

Figure 1 shows the simulation setups of ANSYS-CFX solver. The ANSYS-CFX workbench is the main part of set up all the simulation work. This workbench is an automatic front finite element analysis tool that work with Design Modeler or CAD software. It focuses on

geometry creation and optimization, attaching existing geometry, setting up the finite element model, solving and presenting results. This software also will define the processes conducted, basic finite element simulation concepts and result interpretation [21,22]. The dart paper plane airflow field is solved in 3D, steady state, incompressible and turbulent flow boundary conditions. It is defined based on the Reynolds-average Navier Stokes (RANS) equations are coupled with the Shear Stress Transport (SST) k-ω turbulent model to obtain laminar-turbulent transition region. ANSYS-CFX is utilized the governing equations of the finite volume method together with fully implicit descretization equation to elucidate the CFD computational domain. The precise flow quantifications through CFD simulation over a paper plane can allocate details of aerodynamic characterization and flow structures.

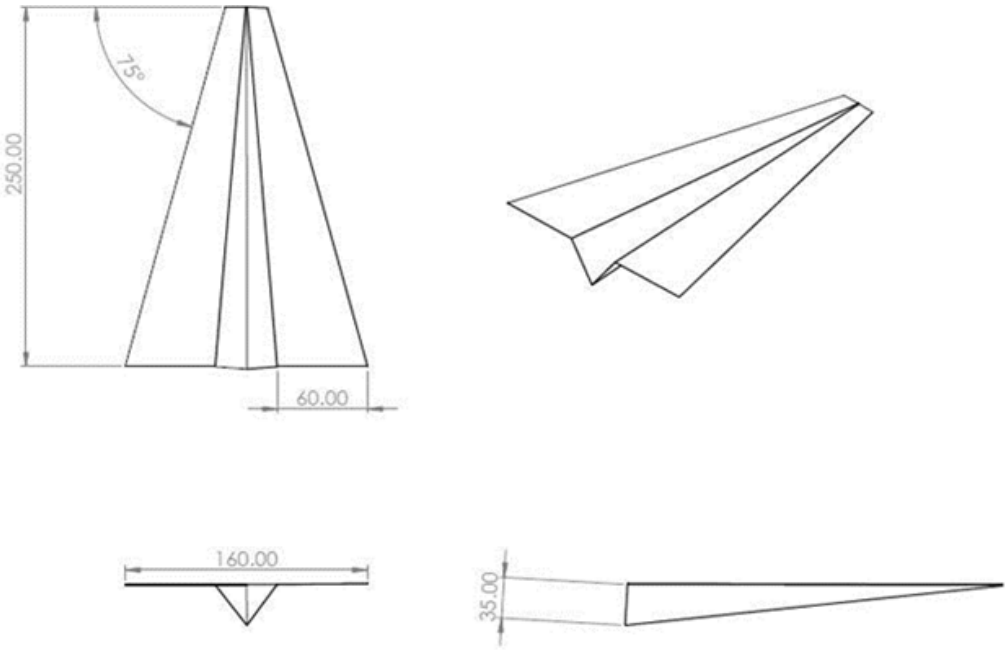

Figure 2: Geometric of Paper Plane Model in millimeter (mm)

For designing the dart paper plane model, SolidWorks software is used. The geometric design of dart paper plane model is shown in Figure 2 which measured in millimeter (mm). SolidWorks is one of a Computer Aided Design (CAD) software is used for modelling a 3D model design. The sheet metal features exist in this software are suitable to use since it required a simple bending process. The bending edge profile on the model is consistent and followed the standard origami technique when built a model. The configuration utilize in this study is based on the experimental model provided by Schlüter, which is a common delta wing paper plane configuration [23]. The paper plane has the root chord length 250 mm and sweep angle of 75° . The CAD model are created and export with Parasolid extension to be dealt with the ANSYS-Design Modeler module. ANSYS-Designer Modeler is used to create and modify the geometry of existing CAD model and their relative cross section for 3D paper plane development. The parametric geometry, concept model creation and CAD geometry modification also being assist in this module**.** In this section**,** the 3D paper plane geometrical model is influenced the flow domain surroundings the paper plane throughout its proportioned dimension as shown in Figure 3 which measured in millimeter (mm). It is provide the schematic view of progressed dart paper plane model enclosed within its surrounding flow domain.

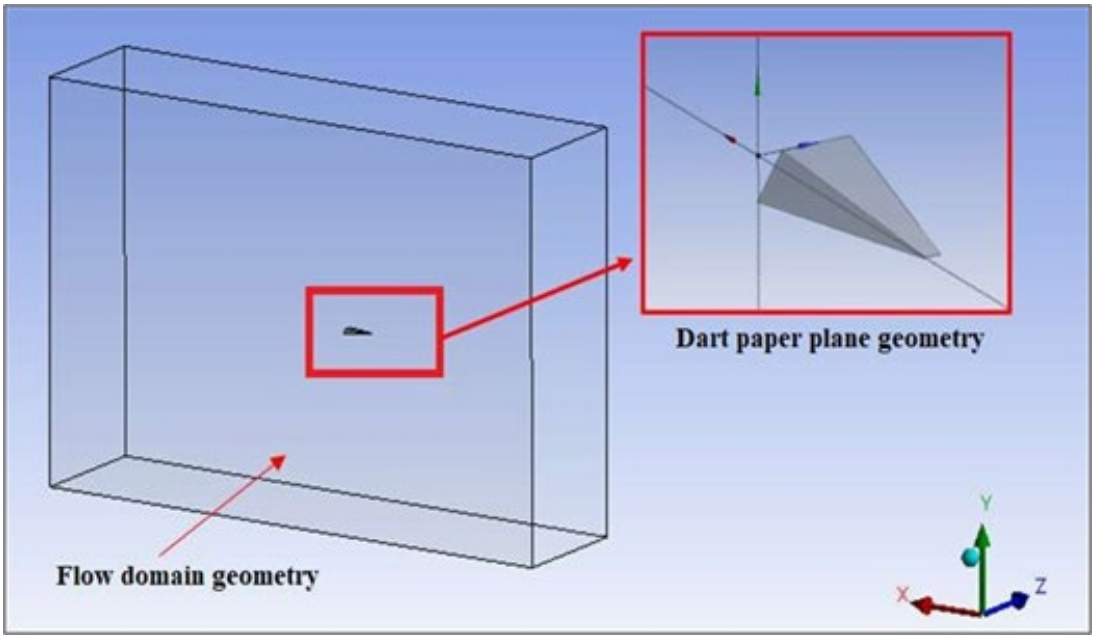

Figure 3: Geometrical of dart paper plane and it is surrounding flow domain

The computational domains set surrounding the paper plane is shown in Figure 4. In recent work, the boundary condition consists of inlet, outlet and symmetrical wall. The flow vectors in ANSYS-CFX setup are used to shows the boundary conditions for the inlet and outlet flows domain wall. The flow vectors which elucidate the direction into the flow domains are denotes as the inlet while the flow vectors pointed outward is the outlet boundary conditions. The symmetrical wall is identified by red marks on the vertical sidewall.

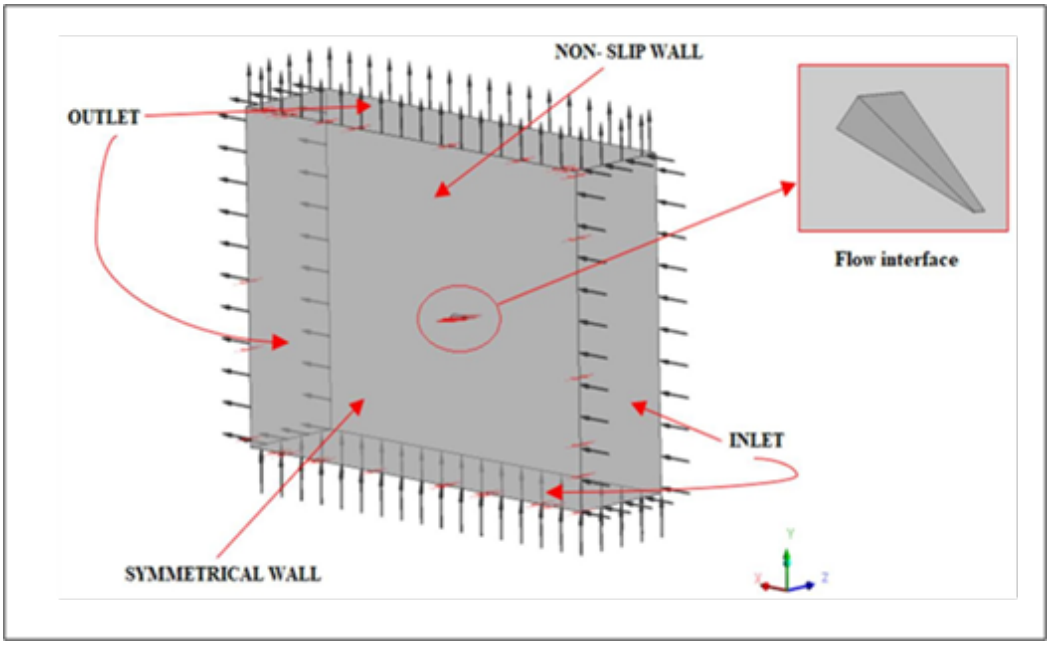

Figure 4: Computational domain boundary condition in ANSYS-CFX Solver

2.2 Mesh Characteristic

In mesh section, CFX-Pre Meshing in ANSYS CFX module is used for creating the hybrid instructed 3D CFD mesh. This module was chosen in present work due to the simpler mesh development to discretize the flow domain. The hybrid mesh has cover of tetrahedral, hexahedral, pyramidal or the prismatic elements [13]. Basically, Patch Conforming Algorithm and inflation

layers are implemented to increase the density of the mesh near the paper plane and inclined surface to seize all the flow features. The y+ value is used for inflation layer aids to capture the mesh information needed with the appropriate refinement normal to the wall. This value is the most importance factor in determinant of activating the correct near wall function. The y+ value obtained for the current mesh CFD work is 0.88. These value are corresponding to the required condition of (y+ < 1) to activate the linear sub-layer function for elucidate the near wall turbulent flow [14]. Besides, a mesh independent study is carried out for this research work for ensuring the suitable mesh number and evaluate the numerical mesh grid quality.

2.3 Fluid Properties and Flow Boundary Conditions

In the current works, the CFD simulations of paper plane are performed with the fluid properties of ideal gas at 25º C. This is due to the suitable temperature for tropical atmospheric conditions at sea level altitude. The constant composition was assumed to be dry and clean, thus it can be work to imitate the same atmospheric condition are used in wind tunnel experiment. Table 2 show the features of Air properties at 25º C.

Table 2: Air Properties at 25º C

Properties	Value
Dynamic Viscosity	1.831×10^{-5} Pa.s
Density	1.185 kg/m^3
Reference Pressure	1 atm

For the flow boundary conditions, the inlet velocity is imposed on the inlet wall, while a zero-pressure boundary conditions enforced at the outlet. The paper plane wing is performed with the uniform freestream velocity of **U**= 5m/s. This is corresponded to Reynolds number based on chord length of *Re* =80,000 at AOA ranging from 0º until 40º. The symmetrical and slip surface boundary conditions in the domain setup are set to define the symmetrical wall and sidewall. Meanwhile, the whole wetted surface on the paper plane wing are defined as no slip boundary conditions layer for ensuring the tangential fluid velocity component at the wing surface equal the velocity on the wall.

2.4 Post Processing Setup

In order to characterize the dart paper plane performance, CFD simulations has makes it easier to formulate aerodynamic parameter such as lift and drag. Therefore, the Lift Coefficient (C_L) and Drag Coefficient (C_D) are expressed by equations below:

$$C_L = \frac{L}{\frac{1}{2}\rho U^2 S} \quad (1)$$

$$C_D = \frac{D}{\frac{1}{2}\rho U^2 S} \quad (2)$$

Where

L= Total lift force
D= Total drag force
ρ= Density
U= Freestream velocity at inlet
S = Wing planform area

The aerodynamic efficiency can derive based on lift and drag performance: It is to measure the parameters of the airplane that can travel during flying through the air. The greater the value of the L/D ratio, the better for design needed for aerodynamic efficiency.

$$\varepsilon = \frac{L}{D} \tag{3}$$

3.0 RESULTS AND DISCUSSION

3.1 Lift Performance

Figure 5 present the overall results of the lift performance (C_L) dart paper plane between the previous simulation and experimental works provided from references [6]. The result also compared with the lift performance of current research works. In overall, the result shows lift coefficient (C_L) for dart paper plane in the pre- stall angle (start from zero until stall angle) has increase linearly with the angle of attack (AOA) increment until it reached their maximum lift coefficient magnitude (C_{Lmax}). However, the C_L magnitude begins to deteriorate with the increment value of AOA after the point of stall angle (AOA_{stall}).

In general, the experimental and simulation results from the previous study are utilized to examine the overall paper plane performance. For this research, there are several characteristics of lift coefficient being focused such as the magnitude lift coefficient ($C_{Lmagnitude}$), stall angle (AOA_{stall}) and lift increment (C_{Lincre}). The magnitude of C_{Lmax} is the maximum point which the lift distribution generated by paper plane. The AOA_{stall} is the stall angle which located at the peak of C_L curve. While the C_{Lincre} magnitude was analyzed at three difference range which is taken at AOA= 0º to 10º, 12º to 20º and 22º to stall of the C_L magnitudes.

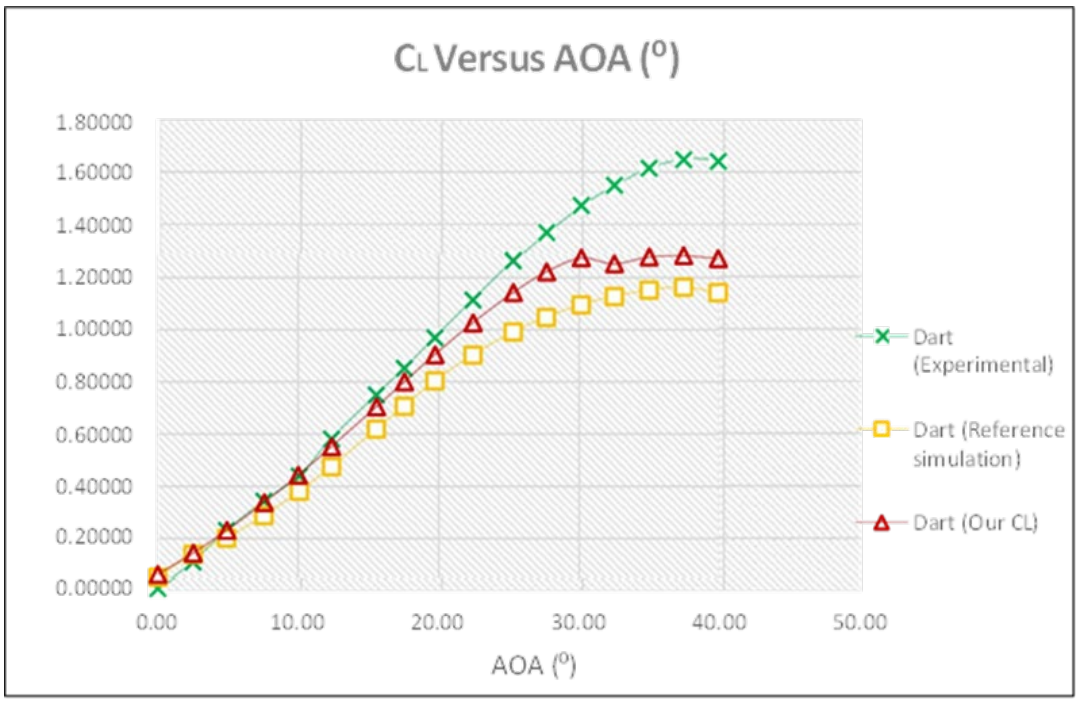

Figure 5: Lift Coefficients (C_L) results of research study

For the lift coefficient magnitude between experimental and our C_L case, the observation in shows both results have a similar non -linear pattern of C_L curved towards the change angle of attack. The results show the experimental results has more obvious non-linear pattern than our C_L. The comparison of $C_{Lmagnitude}$ between experimental and simulation works is analyze at the pre-stall region (AOA< stall angle) which is at AOA = 0º to 10º, 12º to 20º and 22º until stall.

Based on the analysis of magnitude taken at AOA between 0º to 10º, the result for average percentage difference for the $C_{Lmagnitude}$ is 5%. The results show that, at this region our C_L has produce the larger $C_{Lmagnitude}$ distribution than the experimental works. At AOA between 12º to 20º, the difference in percentage between experimental and our C_L start to increase up to 6.6%. This

increment trend continues at AOA 22º until 30º where the average percentage difference value is 11.9%. Here the $C_{Lmagnitude}$ distribution for experimental results clearly higher than our C_L towards the AOA changes.

Meanwhile, C_L magnitude between the simulation result versus our C_L result shows that our C_L works has higher non-linear pattern than the reference simulation [24]. The analysis for the $C_{Lmagnitude}$ and C_{Lincre} for both simulation results are identified at the three differences pre-stall region which is AOA from 0º to 10º, 12º to 20º and 22º to 30º. The AOA_{stall} was analysis based on the C_{Lmax} occurrence. Based on the analysis of magnitude lift coefficient value at AOA 0º to 10º, the average percentage difference between the simulation and our C_L results is 10.5%. Followed by at AOA 12º to 20º, the percentage in $C_{Lmagnitude}$ is 12.1% and 13.3% at AOA 22º to 30º. The results show that our C_L has the higher C_L magnitude in change of AOA increment than reference simulation result.

3.2 Drag Performance

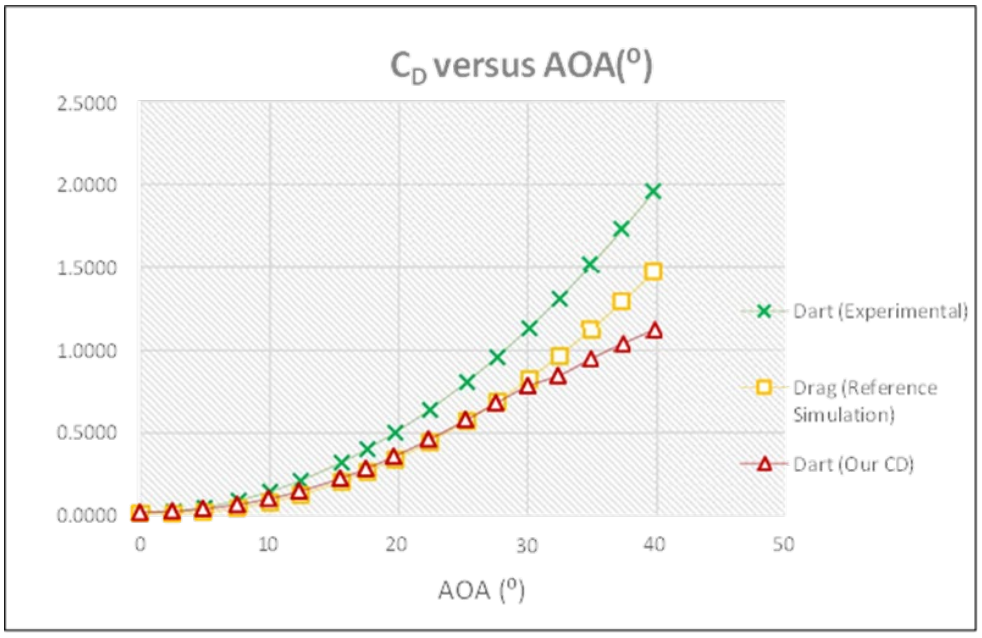

Figure 6: Drag Coefficient (C_D) Results Versus AOA

Figure 6 shows comparison study in Drag Coefficient (C_D) results for experimental and simulation. The graph presents the C_D experimental and simulation data taken from the references work [6] and compared with our C_D results. In overall, one can presumed that the result from all sources produces the similar C_D trend toward the increment of angle of attack (AOA). In this analysis, there are several parts which will be highlighted to examine the overall C_D performance of dart paper plane particularly at pre-stall region (AOA<stall angle) focusing on AOA 0º to 10º, 12º to 20º and 22º until 30º regions. In order to analyze the C_D performance, there are several magnitudes will be discussed at the upcoming text which focusing on C_D magnitude ($C_{Dmagnitude}$) and average drag increment (C_{Dincre}) towards the AOA changes.

Comparison of C_D experimental [6] and our C_D simulation result shows that both results consistently produces an increment of C_D magnitude towards changes of AOA. At low AOA region (0º to 10º), the average percentage difference of the $C_{Dmagnitude}$ between experimental and our C_D simulation is about 25.6%. At the region AOA between 12º to 20º, average percentage difference in $C_{Dmagnitude}$ has been increased up to 41.9%. However, such trend slightly decreased to 41% at AOA between 22º to 30º. In terms of the C_{Dincre} magnitude analysis, at low region (AOA 0º to 10º) the experimental results have produced the average magnitude increment C_{Dincre}= 81.7% which is higher than our C_D results which is about C_{Dincre}= 60.2%. At AOA 12º to 20º, the C_{Dincre} between experimental and our C_D results is 37.1% and 37.8%. At AOA 22º to 30º, the C_{Dincre} for experimental

and our C_D results continue to reduce at 22.7% and 21.8%, respectively. Based on this average magnitude of C_{Dincre} analysis, it can assume that as AOA values increase between AOA 0º to 30º, the average percentage difference of the C_{Dincre} become more explicit from 21.5% to 0.9%, respectively.

In terms of $C_{Dmagnitude}$, the average percentage difference between AOA 0º to 10º for reference simulation and our C_D results is 37.3%. At AOA 12º to 20º, the average percentage difference of the $C_{Dmagnitude}$ is about 9.9% and continuously reduced to 0.3% as AOA increase up to 30º. For the comparison between C_D experimental [6] and our C_D simulation result, both results consistently produces an increment of C_D magnitude towards changes of AOA. At low AOA region (0º to 10º), the average percentage difference of the $C_{Dmagnitude}$ between experimental and our C_D simulation is about 25.6%. At the region AOA between 12º to 20º, average percentage difference in $C_{Dmagnitude}$ has been increased up to 41.9%. However, such trend slightly decreased to 41% at AOA between 22º to 30º. The comparison of C_D magnitude between both results shows that the percentage difference has been increased toward the AOA changes. In terms of the C_{Dincre} magnitude analysis, at low region (AOA 0º to 10º) the experimental results have produced the average magnitude increment C_{Dincre}= 81.7% which is higher than our C_D results which is about C_{Dincre}= 60.2%. At AOA 12º to 20º, the C_{Dincre} between experimental and our C_D results is 37.1% and 37.8%. At AOA 22º to 30º, the C_{Dincre} for experimental and our C_D results continue to reduce at 22.7% and 21.8%, respectively.

As a conclusion, both results have a good correlation particularly for the C_{Dincre}. The average percentage difference has proved that both results approximately has good correlation in terms of C_{Dincre}. However, there are slight differences found in $C_{Dmagnitude}$ between the experimental and our C_D result. This difference might be due to the insufficient to capture skin friction drag in transition phenomenon during the simulation works [24]. In addition, the overall C_D distribution for reference simulation and our C_D results has slightly difference in $C_{Dmagnitude}$. The difference might due to the finite-volume formulation of incompressible Navier-Stokes equations which our C_D result has used steady state while reference simulation used the unsteady state conditions [6]. From the results, we can presume that our C_D results satisfactorily verified with the C_D of reference simulation.

3.3 Aerodynamic Efficiency

The investigation of the aerodynamic performance for dart paper plane is continued by analysis the aerodynamic efficiency. Commonly, the study of the aerodynamic efficiency always refers to the magnitude of lift-to-drag ratio (C_L/C_D). Figure 7 shows the C_L/C_D results for the experimental, reference simulation and our C_L/C_D. The results demonstrate that C_L/C_D curve increase linearly at the early stage (AOA <5º) and began to decrease (AOA > 5º) as the increment of angle of attack (AOA). The main characteristics of this aerodynamic study is the maximum point (C_L/C_{Dmax}) of the aerodynamic efficiency and average percentage difference in angle magnitude.

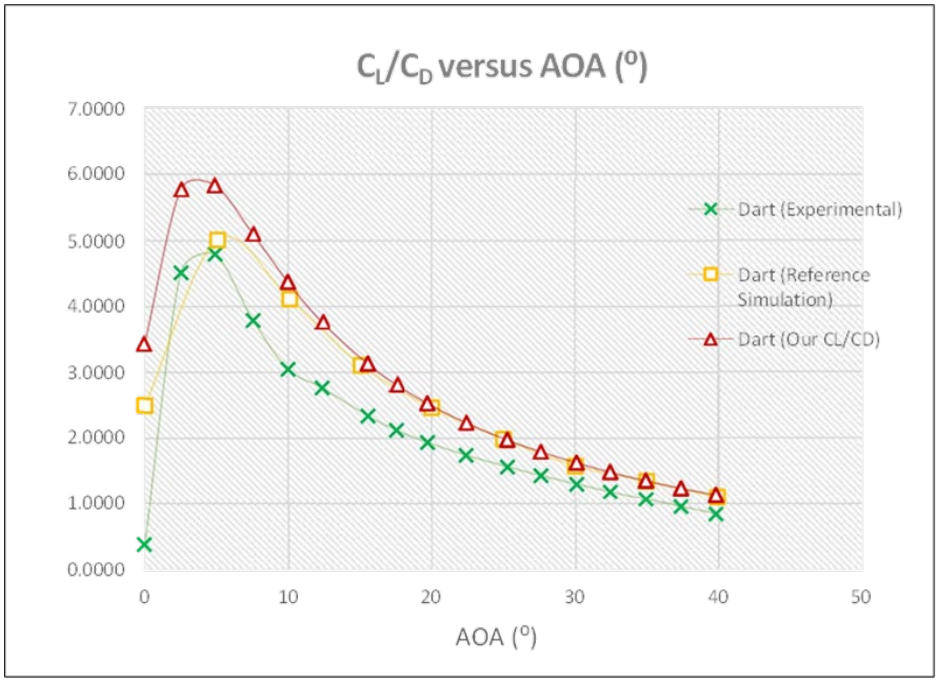

Figure 7: Efficiency of Dart Paper Plane

The results for aerodynamic efficiency between experimental and C_L/C_D results show the nonlinear curve toward the variations of angle of attack (AOA). Based on observation, our C_L/C_D results show the higher magnitude distribution than the experimental. Analysis of CL/C_{Dmax} performance shows that the experimental result experienced the maximum magnitude value of C_L/C_{Dmax} =4.7951 while our C_L/C_D produces C_L/C_{Dmax} =5.8377. The percentage difference of C_L/C_{Dmax} magnitude is about 33.2%. Both results have experienced similar of C_L/C_{Dmax} angle which is at 4.91º.From the analysis, we can conclude that the experimental and our C_L/C_D results experienced almost similar C_L/C_{Dmax} at early AOA stage between 1º to 5º. However, there are huge difference between the experimental and our C_L/C_D results in terms of magnitude might be due to the difference of C_D value at the higher local AOA of the centerfolds that will resulting the lift-to-drag ratio [15].

In overall, the validation works has been done by focusing on the aerodynamic performance such as C_L, C_D and C_L/C_D. Based on the C_L performance, the results show that experimental has produce the higher of the $C_{Lmagnitude}$ towards the increment of AOA compared to the reference simulation and our CL results. However, the experimental and reference simulation show a delayed AOA_{stall} and C_{Lmax} magnitude than our C_L results. For the increment of magnitude distribution for every result at the pre stall region show it has exhibit similar C_{Lincre} towards the change of AOA. Based on C_D performance, it is apparently show C_D magnitude for every result had increase towards the change of AOA. The C_{Dincre} at the pre stall region for every magnitude distribution has reduced and satisfactorily verified. The detailed of C_L/C_{Dmax} shows that our results had the highest C_L/C_{Dmax} magnitude which about 5.8377 at AOA 5º. This percentage magnitude difference from the experimental and references simulation is about 33.2% and 16.5%. The difference might be due to the C_D magnitude which consequently lowered overall C_L/C_D performances.

4.0 CONCLUSION

The research presents CFD analysis of the aerodynamic performance characterization which focused on the basic aerodynamic performance (C_L, C_D, C_L/C_D). CFX simulation is the main methodology used to analyze flow system of 3D dart paper plane model based on the steady state and incompressible RANS-SST turbulence flow. The availability of the experimental data is used to support the aerodynamic validations works. Based on the lift performance analysis, the

magnitude distribution of our simulation and experimental result reveals a good correlation especially at pre-stall region. Only slightly difference found in terms of $C_{Lmagnitude}$, C_{Lmax} and AOA_{stall} which the highest average percentage difference between each result is 11.9%, 29.5% and 24.2%. Despite having a difference of magnitude distribution during the validation work, the overall aerodynamic trends of the C_L curve pattern are similarly exhibited since the average percentage difference of the C_{Lincre} at the pre-stall region has continuously reduce from 6.48% until 0.9% towards increment of AOA. In terms of drag performance analysis, the overall trends magnitude distribution of our simulation and experimental results are consistently increase towards the increment of AOA. This is because both results have shown good correlation particularly based on the C_{Dincre}. Based on the aerodynamic efficiency analysis, our simulation results had similarly experienced the C_L/C_{Dmax} at the early AOA stages with the experimental results which at 4.91º. However, in terms of magnitude our simulation results have generate 33.2% higher than experimental results. The difference is due to the experimental result has generates huge C_D magnitudes, thus will decrease the C_L/C_{Dmax} magnitude on dart paper plane.

ACKNOWLEDGEMENTS

The author expresses gratitude to UTM for assisting students in conducting this research. Sincere thanks also go to colleagues and individuals who have supported me on different occasions. Their insights and advice have been invaluable, although it's impractical to mention everyone here. Appreciation is also extended to family members.

REFERENCES

1. Choi, K. H. (2016). Practice-led origami-inspired fashion design: out of the frame: flight by paper plane. International Journal of Fashion Design, Technology and Education, *9*(3), 210-221. doi: 10.1080/17543266.2016.1158872.
2. Pounds, P. (2012). Paper plane: Towards disposable low-cost folded cellulose-substrate UAVs. In Australasian Conference on Robotics and Automation (pp. 3-5).
3. Ng, B. F., Kng, Q. M., Pey, Y. Y., & Schluter, J. (2009, June). On the aerodynamics of paper airplanes. In *27th AIAA applied aerodynamics conference* (p. 3958). doi: 10.2514/6.2009-3958.
4. N. I. Ismail, M. K. Khadzali, R. J. Talib, and Z. M. Ali, (2016). The Lift and Drag Performance of Paper Planes, in Mechanical Engineering Colloquium (MEC 2016), pp. 22–27.
5. Mueller, T. J. (Ed.). (2001). Fixed and flapping wing aerodynamics for micro air vehicle applications. American Institute of Aeronautics and Astronautics, pp. 1–10. doi: 10.2514/4.866654.
6. Gurnani, S., & Damodaran, M. (2019). Computational aeromechanics of paper airplanes. Journal of Aircraft, 56(5), 2070-2079. doi: 10.2514/1.C035339.
7. Ismail, N. I., Sharudin, H., Talib, R. J., Hassan, A. A., & Yusoff, H. (2018, May). The Influence of Hoop Diameter on Aerodynamic Performance of O-Ring Paper Plane. In IOP Conference Series: Materials Science and Engineering (Vol. 370, No. 1, p. 012034). IOP Publishing. doi: 10.1088/1757-899X/370/1/012034.
8. Schlueter, J. U. (2014). Aerodynamic study of the dart paper airplane for micro air vehicle application. Proceedings of the Institution of Mechanical Engineers, Part G: Journal of Aerospace Engineering, 228(4), 567-576. doi: 10.1177/0954410013476778.
9. Chang, M., Feng, X., Zhang, Y., Zhang, X., & Bai, J. (2023). Flow analysis on the ventral gap of a paper airplane. Proceedings of the Institution of Mechanical Engineers, Part C: Journal of Mechanical Engineering Science, 237(18), 4131-4140. doi: 10.1177/0954406220946076.
10. Ismail, N. I., Zulkifli, A. H., Basri, M. H., Talib, R. J., & Yusoff, H. (2015). Lift performance of a twist morphing MAV wing. *Jurnal Teknologi*, *75*(8). doi: 10.11113/jt.v75.5206.
11. N. Cook, (2017), Experimental analysis of paper plane flight characteristics (Master's thesis), University of Queensland.
12. Collins, J. M. (2013). The new world champion paper airplane book: Featuring the world record-breaking design, with tear-out planes to fold and fly. Ten Speed Press.
13. Gabriel, E. T., & Mueller, T. J. (2004). Low-aspect-ratio wing aerodynamics at low Reynolds number. AIAA J, 42(5), 865-873. doi: 10.2514/1.439.
14. Cosyn, P., & Vierendeels, J. (2006). Numerical investigation of low-aspect-ratio wings at low Reynolds numbers. Journal of Aircraft, 43(3), 713-722. doi: 10.2514/1.16991
15. Harbig, R. R., Sheridan, J., & Thompson, M. C. (2013). Reynolds number and aspect ratio effects on the leading-edge vortex for rotating insect wing planforms. Journal of Fluid Mechanics, 717, 166-192. doi: 10.1017/jfm.2012.565.

16. Ng, B. F., Kng, Q. M., Pey, Y. Y., & Schluter, J. (2009, June). On the aerodynamics of paper airplanes. In *27th AIAA applied aerodynamics conference* (p. 3958).
17. Zhang, Y., Zhang, X., & Chen, G. (2021). The aerodynamic optimisation of a low-Reynolds paper plane with adjoint method. *The Aeronautical Journal*, *125*(1285), 510-524. doi:10.1017/aer.2020.78
18. Sibilski, K., Nowakowski, M., Rykaczewski, D., Szczepaniak, P., Żyluk, A., Sibilska-Mroziewicz, A., ... & Wróblewski, W. (2020). Identification of fixed-wing micro aerial vehicle aerodynamic derivatives from dynamic water tunnel tests. *Aerospace*, *7*(8), 116. doi:10.3390/aerospace7080116
19. Kumar, O. (2022). Aerodynamics Performance Of Fixed Wing Micro Air Vehicle With Different Planforms.
20. Rajanna, M. R., Johnson, E. L., Codoni, D., Korobenko, A., Bazilevs, Y., Liu, N., ... & Hsu, M. C. (2022). Finite element methodology for modeling aircraft aerodynamics: development, simulation, and validation. *Computational Mechanics*, *70*(3), 549-563. doi.org/10.1007/s00466-022-02178-7
21. Ismail, N. I., Ali, Z. M., Ishak, I. S., Noor, R. M., & Rabilah, R. (2021). Aerodynamic performances of paper planes. *Journal of Advanced Research in Fluid Mechanics and Thermal Sciences*, *77*(1), 124-131. doi.org/10.37934/arfmts.77.1.124131
22. Liu, D., Song, B., Yang, W., Yang, X., Xue, D., & Lang, X. (2021). A brief review on aerodynamic performance of wingtip slots and research prospect. *Journal of Bionic Engineering*, *18*, 1255-1279. doi.org/10.1007/s42235-021-00116-6
23. Cook, N. (2017). Experimental analysis of paper plane flight characteristics.
24. Ma, P. (2024). Experimental Study and Analysis of Aerodynamic Characteristics of Gliders with Different Wing Geometries. *Highlights in Science, Engineering and Technology*, *93*, 76-81. doi.org/10.54097/3mv6ge22